

# REGAL: Transfer Learning For Fast Optimization of Computation Graphs

Aditya Paliwal\*  
Google Research  
adipal@google.com

Yujia Li  
DeepMind  
yujiali@google.com

Felix Gimeno  
DeepMind  
fgimeno@google.com

Miles Lubin  
Google Research  
mlubin@google.com

Oriol Vinyals  
DeepMind  
vinyals@google.com

Vinod Nair  
DeepMind  
vinair@google.com

Pushmeet Kohli  
DeepMind  
pushmeet@google.com

## ABSTRACT

We present a deep reinforcement learning approach to optimizing the execution cost of computation graphs in a static compiler. The key idea is to combine a neural network policy with a genetic algorithm, the Biased Random-Key Genetic Algorithm (BRKGA). The policy is trained to predict, given an input graph to be optimized, the node-level probability distributions for sampling mutations and crossovers in BRKGA. Our approach, “REINFORCE-based Genetic Algorithm Learning” (REGAL), uses the policy’s ability to transfer to new graphs to significantly improve the solution quality of the genetic algorithm for the same objective evaluation budget. As a concrete application, we show results for minimizing peak memory in TensorFlow graphs by jointly optimizing device placement and scheduling. REGAL achieves on average 3.56% lower peak memory than BRKGA on previously unseen graphs, outperforming all the algorithms we compare to, and giving 4.4× bigger improvement than the next best algorithm. We also evaluate REGAL on a production compiler team’s performance benchmark of XLA graphs and achieve on average 3.74% lower peak memory than BRKGA, again outperforming all others. Our approach and analysis is made possible by collecting a dataset of 372 unique real-world TensorFlow graphs, more than an order of magnitude more data than previous work.

## KEYWORDS

reinforcement learning, genetic algorithms, task scheduling, graph neural networks

## 1 INTRODUCTION

Deep Learning frameworks such as TensorFlow [2], PyTorch [25], and MXNet [6] represent neural network models as computation graphs. There is growing interest in using static compilers to improve performance of executing these computation graphs and to access specialized hardware; see e.g., XLA [30], Glow [26], and TVM [7]. Such a static compiler makes a large number of discrete decisions that determine various execution costs of a graph, such as running time and peak memory usage. For example, it may decide which nodes in a graph are executed on which device (the “device

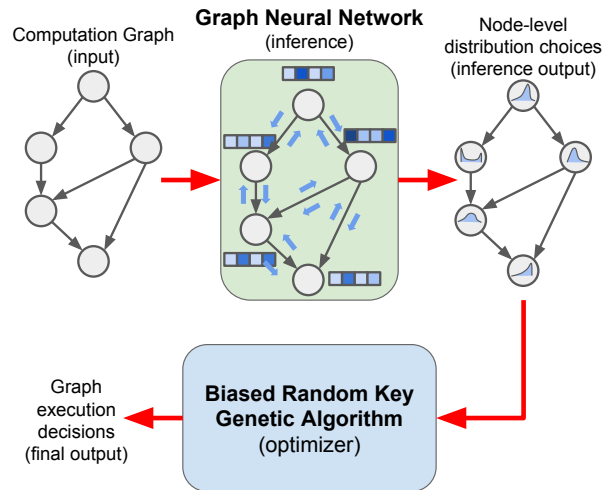


Figure 1: Overview of REGAL.

placement” problem [22]), and the per-device order in which nodes are executed (scheduling). The resulting high-dimensional combinatorial optimization problems have been studied as *task scheduling*, which is known to be NP-hard in typical settings [18, 29]. Despite the difficulty of the decisions to be made, static compilers are expected to produce good solutions quickly.

In this work, we use machine learning to optimize the execution cost of computation graphs. Learning approaches enable *learning a custom optimizer* for the distribution of graphs relevant to a specific application. By *transferring* or *generalizing* to new samples from the same distribution, a learned optimizer can solve them better than a generic one [3].

Our optimizers solve a mathematical optimization problem (i.e., minimizing an objective function) applied to improving performance of computation graphs (in the sense that a compiler optimizes computer programs). These computation graphs to which we apply the optimizers often represent neural networks on which gradient descent, an optimization algorithm, is performed. To learn the parameters of our custom optimizers, we use REINFORCE, another optimization algorithm. It’s optimization *all the way down*.

\* Google AI Resident

We demonstrate the efficacy of our novel learning-to-optimize framework by applying it on the Biased Random-Key Genetic Algorithm (BRKGA, section 3.2), which has been successful in a wide array of hard combinatorial optimization problems [12]. We aim to improve BRKGA’s solution quality for the execution decisions of computation graphs via learning. The key idea is to train a neural network policy that takes a computation graph as input and proposes distributions to use in the mutation and crossover steps of BRKGA’s inner loop. The distributions are predicted at each node in the graph, resulting in a high-dimensional prediction problem. There is no explicit supervision available except for the objective value as a reward signal, so learning a good policy involves a hard explore-exploit problem. We use a contextual bandit approach with REINFORCE [31] to learn the policy (section 3.4). Our proposal, “REINFORCE-based Genetic Algorithm Learning” (**REGAL**), parameterizes the policy as a graph neural network [10] to use the graph structure of the input (section 3.3).

Figure 1 gives an overview of how the trained network is used at test time. Given a new graph, the graph neural network predicts node-level distribution choices to be used by BRKGA. BRKGA is then run to completion with those choices, instead of using the input-agnostic default choices in the original BRKGA formulation [12]. By the network’s ability to transfer, on seeing a new graph it can predict choices that give better solution quality than the default ones. Transfer avoids having to train a separate neural network for each new graph, which can take hours [22]. Instead, the time to run the optimizer is the time to run the inference pass of the graph neural network policy and the time to run BRKGA, both of which takes only seconds (see table 2).

To demonstrate our approach, we select the problem of jointly optimizing the placement and schedule for computation graphs on multiple devices. As users design bigger neural network models to achieve better task performance, a model often does not fit into one device. *Model parallelism*, splitting a single model across multiple devices, becomes necessary to scale to larger models. Our work aims to improve the computational cost of model parallelism.

In our application, a production compiler needs to deal with a broad set of users who define a diverse set of graphs. So the learned policy must generalize broadly. To ensure this, we collect a dataset of 372 real-world TensorFlow graphs created by users (section 4.1). We show that a policy trained on this dataset (with augmentation) is able to successfully generalize to previously unseen graphs (sections 4.3, 4.4).

We choose peak memory usage of a graph as the performance objective to be minimized (section 3.1). Peak memory determines the size of the largest neural network that fits into memory, so it can have significant impact on task performance by making larger networks feasible to run. Our approach is not specific to any one objective, and other objectives, e.g., running time, could also have been used. Examples of other important decisions in static compilers that our work could be extended to address are fusing ops [4], and recomputing tensors instead of storing them to trade-off speed and memory [8].

We use BRKGA because it is fast and its node-level distribution choices provide a rich set of targets to be learned. For the task we consider, BRKGA can produce solutions of good quality in seconds even on graphs with low thousands of nodes. By predicting

BRKGA’s node-level distributions, the learning problem is made more abstract since the policy does not need to directly predict the optimal solution. We believe such a policy can transfer better to a broader set of graphs at test time.

## 1.1 Contributions

Our key contributions are:

- (1) A novel approach to learning a better performance optimizer for computation graphs. To the best of our knowledge, ours is the first work to show transfer on a broad set of real-world TensorFlow graphs of varying sizes and architectures. It gives a 3.56% reduction in peak memory usage on average of previously unseen TensorFlow graphs, 4.4× better than the next best algorithm (section 4.3). It also gives a 3.74% peak memory reduction on average on a production compiler team’s performance benchmark of XLA graphs, again outperforming all other algorithms.
- (2) We base our approach on Graph Neural Networks, which can effectively utilize the structural information in the computation graphs, and provide the foundation for generalizing across graphs from different sources and of different sizes.
- (3) We evaluate our approach on a dataset of 372 topologically distinct real-world TensorFlow graphs collected from research and production use cases, which is an order of magnitude larger than the datasets used by previous works [1, 9, 21, 22].
- (4) We perform extensive comparisons to baselines, covering evolutionary search, local search, constraint programming, and alternative learning-based approaches.

## 2 RELATED WORK

*Learning to optimize computation graphs:* Existing work in the context of Deep Learning frameworks either does not attempt transfer to new graphs [21, 22], or have shown only limited transfer [1, 7]. In [21, 22] learning is done from scratch for each computation graph, which requires hours (e.g., 12 to 27 hours per graph [22]). Our use case allows only seconds to tens of seconds for similarly sized graphs. AutoTVM [7] shows results for transferring to previously unseen hyperparameter settings for a single neural network model, ResNet-18, but they do not attempt transfer across different models. Placeto [1] learns a policy for a single model, Inception-V3, and uses it to initialize the training of policies for another model, resulting in less training time to achieve the same solution quality. We go one step further and fully remove the need for training on a new model. Our work can also be seen as an instance of applying machine learning for combinatorial optimization [3].

*Learning a proposal distribution for stochastic search:* Our work is closest in spirit to [5] which learns a policy for predicting instance-dependent proposal distributions to be used in the stochastic optimizer STOKE [28] for superoptimizing programs. However, it uses handcrafted instance features and shows results on relatively simple, small programs. In contrast, we automatically learn the instance representations and show results on real-world graphs. An earlier work [23] similarly learns a neural network to predict input-dependent proposal distributions for sequential Monte Carlo search for inference in a graphical model.

*Optimization without learning:* Parallel task scheduling [18, 29] is a classical problem for scheduling ops in a computational graph to minimize runtime. Learning is not traditionally a part of the approaches proposed in this literature. [15] develops an effective simulation-based optimizer for deep learning computation graphs.

### 3 APPROACH

Figure 2 shows an overview of the pipeline for our approach. The next three subsections explain its key components in more detail.

#### 3.1 The multi-device peak memory minimization problem

We formally describe our model for computation graphs and the peak memory minimization objective and then note a few of its limitations.

The scheduling problem is specified by a set of devices  $D$  and a computation graph. The computation graph has the list of ops  $j \in N$  and tensors  $\tau \in T$ , the tensors produced by each op  $I(j) \subseteq T$ , the tensors consumed by  $C(j) \subseteq T$ , and the memory used by each tensor  $m_\tau$ . A tensor is produced by exactly one op but can be consumed by many.

Solutions to the scheduling problem are constructed as follows. A placement is an assignment  $pl : N \rightarrow D$  from ops to devices. Given a placement we define  $\tilde{N}_{pl}$  as the set of ops  $N$  extended with synchronous inter-device transfer operations. A transfer operation consumes a tensor on the device where it was created and produces it on a device where it is needed.

Given a placement  $pl$ , a schedule is a total ordering  $s : \tilde{N} \rightarrow \{1, 2, \dots, |\tilde{N}|\}$  on ops in  $\tilde{N}_{pl}$ . We say that op  $j$  runs at time  $s(j)$ . We model the schedule execution as follows. At each time step  $t \in \{1, 2, \dots, |\tilde{N}|\}$ , each device  $d$  has a list  $l_{d,t}$  of tensors currently in memory. A tensor is added to the list when produced by an op that runs on the device or by a transfer op that receives the tensor on the device. A tensor is removed immediately after all of its consumers on the device have run. A schedule is valid if for each op  $j$ , all the input tensors are available on the corresponding device at time  $s(j)$ . See Section A.4 for an example schedule.

The memory used on a device at  $t$  is the sum of the memory used by each tensor that is in memory, i.e.,  $\sum_{\tau \in l_{d,t}} m_\tau$ . The peak memory of a schedule is the maximum value of the memory used at any time and on any device. This is the *performance model* in Figure 2.

The scheduling model we consider applies to subblocks of a computation graph without control flow or loops. We do not consider rematerialization of tensors. We also do not account for fragmentation when computing memory use.

#### 3.2 Biased Random-Key Genetic Algorithm

Biased random-key genetic algorithm (BRKGA) is a meta-heuristic framework that has been successful in a wide array of applications for solving hard combinatorial optimization problems [12]. In BRKGA, chromosomes in a population are encoded as  $n$ -dimensional vectors with entries in  $[0, 1]$  for some fixed  $n$ . This *random-key* encoding decouples the application from the genetic algorithm, specifically the crossover and mutant generation procedures. The

goal of BRKGA is to find the chromosome that maximizes a given fitness function.

The BRKGA variant we use is specified by (1) a fitness evaluation function  $f : [0, 1]^n \rightarrow \mathbb{R}$ , (2) scalar integer parameters  $\pi$ ,  $\pi_e$ , and  $\pi_c$  representing the population size, number of elites, and number of children, resp., (3) a vector  $\rho \in [0.5, 1.0]^n$  representing elite biases, and (4) a chromosome generation distribution  $\mathcal{D}$  over  $[0, 1]^n$ .

The initial population (a collection of  $\pi$  chromosomes) is created by sampling from  $\mathcal{D}$ . (Known good solutions may also be used to initialize a population.) A population is evolved as follows.

- (1) Sort the chromosomes in order of decreasing fitness using  $f$ . Denote the first  $\pi_e$  chromosomes as *elites* and the remaining chromosomes as *nonelites*.
- (2) The next generation is constructed from three different sources of chromosomes as follows.
  - (a) Copy the elite chromosomes unmodified from the last generation.
  - (b) For each of the  $\pi_c$  new children, select two parent chromosomes uniformly at random, one from the nonelites and one from the elites. Apply the crossover procedure (described below) to generate a new chromosome given the two parents.
  - (c) Generate the remaining  $\pi - \pi_e - \pi_c$  by sampling from the chromosome generation distribution  $\mathcal{D}$ .

We continue the evolution procedure for a fixed number of evaluations, i.e., calls to  $f$ . Given an elite and nonelite chromosome  $\mathbf{a}, \mathbf{b} \in [0, 1]^n$  (resp.), the crossover procedure produces a child chromosome  $\mathbf{c}$  as follows. For each index  $i \in 1, \dots, n$  independently, let  $c_i = a_i$  with probability  $\rho_i$  and  $c_i = b_i$  with probability  $1 - \rho_i$ .

In standard BRKGA, the chromosome generation distribution  $\mathcal{D}$  is i.i.d. uniform on  $[0, 1]$  and all elements of  $\rho$  are equal. We have generalized BRKGA for instance-specific learning. We replace  $\mathcal{D}$  with  $n$  independent beta distributions (whose parameters can vary by index) and  $\rho$  can also vary by index.

**3.2.1 Chromosome decoding and evaluation.** In order to apply BRKGA to the multi-device peak memory minimization problem, it is sufficient to specify the chromosome dimension  $n$  and the evaluation function  $f$ . The chromosome has three distinct parts:

- (1)  $|N| \times |D|$  entries specifying the affinity of op  $j \in N$  for device  $d \in D \forall (j, d) \in N \times D$
- (2)  $|N|$  entries specifying scheduling priorities for each original op
- (3)  $|T| \times |D|$  entries specifying priorities for transferring tensor  $\tau$  to device  $d$

Given a chromosome, first the placement  $pl$  is constructed by assigning each op to the device with highest affinity. Then we construct the extended set of operations  $\tilde{N}_{pl}$  with transfers included as needed. Each op in  $\tilde{N}_{pl}$  is assigned a priority from the remaining two parts of the chromosome. We then obtain a schedule by performing a topological sort over the operations (with edges defined by data dependencies), breaking ties by using the node priorities, to obtain a total ordering over  $\tilde{N}_{pl}$ . Given a total ordering, we compute the peak memory usage by walking forward in the schedule.

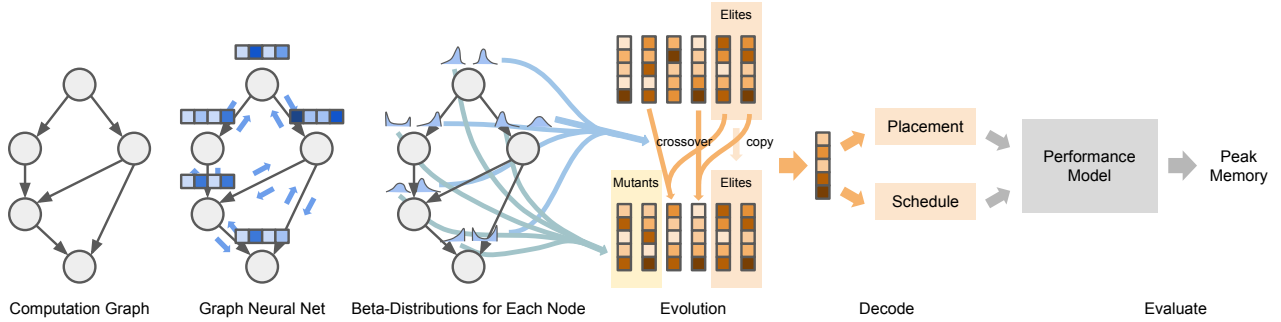


**Figure 2: Our approach for computation graph optimization.** Given an input computation graph, we run graph neural networks on it which uses an iterative message passing procedure to predict a few beta distributions for each node. These beta distributions are then used in BRKGA to generate mutants and decide cross-over probabilities in the evolution process. The optimal chromosome found after evolution is then decoded back into placements and schedules for the computation graph.

### 3.3 Graph neural net architectures

From computation graphs we derive multigraphs with attributed nodes and directed edges. Denote a multigraph  $G = (V, E)$ . In our setup,  $V$  corresponds to the ops, and  $E$  corresponds to the tensors. An edge  $e \in E$  exists from node  $u$  to node  $v$  if node  $v$  depends directly on a tensor produced by  $u$ . It is possible to have multiple edges between two nodes  $u$  and  $v$  as op  $u$  can produce multiple tensors and  $v$  may depend on multiple of them. Each node  $v \in V$  and edge  $e \in E$  have an attribute vector  $\mathbf{x}_v$  and  $\mathbf{x}_e$ . The attributes can contain information about, e.g., sizes of the tensors.

We learn a model that predicts the suitable distribution choices for BRKGA for each computation graph instance. By using a learned model and predicting different parameters for each graph, we can make BRKGA find better solutions faster. Here we consider predicting the parameters of the chromosome generation distribution  $\mathcal{D}$  and the elite biases, which are represented as a vector of parameters  $\mathbf{y}_v$  for each node  $v$ .

We use Graph Neural Networks (GNNs) [10, 11, 20, 27] to learn representations for computation graphs. Given a (multi)graph  $G$ , a GNN computes representation vectors  $\mathbf{h}_v$  for each node through an iterative message passing process as follows:

$$\mathbf{h}_v^{(0)} = \text{MLP}_n(\mathbf{x}_v) \quad (1)$$

$$\mathbf{h}_e = \text{MLP}_e(\mathbf{x}_e) \quad (2)$$

$$\mathbf{m}_e^{(t)} = \text{MLP}_{\text{msg}}([\mathbf{h}_{e_s}^{(t)}, \mathbf{h}_{e_t}^{(t)}, \mathbf{h}_e]) \quad (3)$$

$$\mathbf{m}_e^{(t)'} = \text{MLP}'_{\text{msg}}([\mathbf{h}_{e_s}^{(t)}, \mathbf{h}_{e_t}^{(t)}, \mathbf{h}_e]) \quad (4)$$

$$\mathbf{h}_v^{(t+1)} = \text{MLP}_{\text{node}} \left( \left[ \mathbf{h}_v^{(t)}, \sum_{e: e_t=v} \mathbf{m}_e^{(t)} + \sum_{e: e_s=v} \mathbf{m}_e^{(t)'} \right] \right), \quad (5)$$

where  $e_s$  is the source node of edge  $e$  and  $e_t$  is the target node. We used MLP to represent Multi-Layer Perceptrons, or fully connected neural networks. In our formulation,  $\text{MLP}_n$  and  $\text{MLP}_e$  are MLPs that encode node and edge attributes,  $\text{MLP}_{\text{msg}}$  and  $\text{MLP}'_{\text{msg}}$  computes messages along the edges in the edge direction ( $\mathbf{m}_e^{(t)}$ ) and the opposite direction ( $\mathbf{m}_e^{(t)'}$ ),  $\text{MLP}_{\text{node}}$  updates node representations and  $[\cdot]$  represents flat vector concatenation. After  $T$  rounds of

message passing, the representation for each node  $\mathbf{h}_v = \mathbf{h}_v^{(T)}$  will contain information from the  $T$ -hop neighborhood around  $v$  in the graph. Given the  $\mathbf{h}_v$ 's, we can produce  $\mathbf{y}_v$ 's in a few different ways.

*Conditionally Independent Predictions.* In this approach, we predict  $\mathbf{y}_v$  using  $\mathbf{h}_v$  for each node  $v$  independently:

$$p(\mathbf{y}|G) = \prod_v p(\mathbf{y}_v|G) = \prod_v p(\mathbf{y}_v|\text{MLP}_y(\mathbf{h}_v)). \quad (6)$$

The predictions  $\mathbf{y}$  for different nodes are conditionally independent given the representation vectors  $\mathbf{h}_v$ , and  $\text{MLP}_y$  is shared across all nodes for predicting the parameters of the output distributions. The parameterization of the output distributions is problem dependent. If the outputs are categorical, then  $\text{MLP}_y(\mathbf{h}_v)$  can be the logits of a softmax distribution, and if the outputs are continuous,  $\text{MLP}_y(\mathbf{h}_v)$  can be the mean and variance of the proper distribution family.

This model relies on the representation vectors  $\mathbf{h}_v$  to capture the structure information. However, this model can potentially be further improved by modeling the correlation between outputs.

*Autoregressive Predictions.* We can use an autoregressive model to capture some structure in the outputs. Given the node representations  $\mathbf{h}_v$  for each of the nodes from the GNN, we can utilize an ordering of the nodes, e.g. from a topological sort, and treat the node representations as a sequence, and then use an LSTM [14] to predict the outputs  $\mathbf{y}_v$  sequentially.

We tried this approach but found that using an LSTM on top of the  $\mathbf{h}_v$ 's to predict  $\mathbf{y}_v$ 's did not perform as well as the conditionally independent model. The reasons for this might be: (1) the autoregressive approach relies on a sequential ordering of the nodes, and this ordering might not be reliable nor consistent across graphs; (2) the number of nodes in the computation graphs can be large, and learning recurrent models on long sequences is known to be challenging [24]; (3) the noisy training signal in our REINFORCE-based training setup makes this model even more difficult to train.

*Actions.* In reinforcement learning terms,  $\mathbf{y}$  is a high-dimensional action vector sampled from the policy  $p(\mathbf{y}|G)$ . The sub-action  $\mathbf{y}_v$  at node  $v$  defines the beta distributions and elite bias probability used by BRKGA for that node. We define  $\mathbf{y}$  to be a discrete action vector,

and use a simple linear quantization to map between the (continuous) parameters of beta distributions and elite bias probabilities, and the actions. See details in section A.2.

*Reward.* Once the action vector is dequantized to define node-specific beta distributions and elite bias probabilities, BRKGA is run till completion, and the final objective value is used to compute the reward. To make the reward values comparable across different graphs, we divide the objective value  $o_a(G)$  achieved on a graph  $G$  with action  $a$  by the standard BRKGA’s objective value  $o_s(G)$ . Since we want to minimize the objective (peak memory), we define the reward as  $r = -\frac{o_a(G)}{o_s(G)}$ . So a reward  $> -1$  corresponds to an action that achieves a better objective value than standard BRKGA on a graph.

### 3.4 REINFORCE-based learning

Learning is done by REINFORCE [31]. We maximize the expected reward

$$L = \mathbb{E}_G \left[ \sum_{\mathbf{y}} p(\mathbf{y}|G) r(\mathbf{y}, G) \right], \quad (7)$$

where  $\mathbb{E}_G$  is an expectation over graphs in our training set and  $r(\mathbf{y}, G)$  is the reward obtained by using  $\mathbf{y}$  on  $G$ . The derivative over model parameters  $\theta$  is

$$\frac{\partial L}{\partial \theta} = \mathbb{E}_G \left[ \sum_{\mathbf{y}} p(\mathbf{y}|G) \frac{\partial \log p(\mathbf{y}|G)}{\partial \theta} [r(\mathbf{y}, G) - b(G)] \right]. \quad (8)$$

We added a scalar baseline  $b(G)$  for reducing the variance of the gradient estimates without introducing bias (it is easy to verify that  $\sum_{\mathbf{y}} p(\mathbf{y}|G) \frac{\partial \log p(\mathbf{y}|G)}{\partial \theta} b(G) = 0$  for any  $b(G)$ ). The baseline is computed using a separate GNN, where after we obtained the node representations  $\mathbf{h}_v$ , we compute  $b(G)$  as

$$b(G) = \text{MLP}_b \left( \frac{1}{|V|} \sum_v \text{MLP}_g(\mathbf{h}_v) \right). \quad (9)$$

We use a baseline loss  $\frac{\lambda}{2} (r(\mathbf{y}, G) - b(G))^2$  to train the baseline model. This loss is simply added to the objective (with a negative sign).  $\lambda$  is the weight for this loss.

## 4 EXPERIMENTAL RESULTS

In this section we describe the datasets, the baseline algorithms we compare to, and quantitative results for evaluating REGAL.

### 4.1 Datasets

We have collected a dataset of topologically-unique real-world TensorFlow graphs by mining machine learning jobs that ran on a shared production cluster. The jobs are from a wide range of production and research use cases. We de-duplicate the dataset by graph topology. Figure 3 (left column) gives statistics for the number of nodes and edges in the de-duplicated graphs. The broad range of graph sizes indicates the diversity of the dataset. The resulting 372 unique graphs are split into {train, valid, test} sets as 60%-20%-20% containing {224, 74, 74} graphs, respectively. These sets are disjoint with respect to graph topology, so at test time the policy needs to generalize to new topologies.

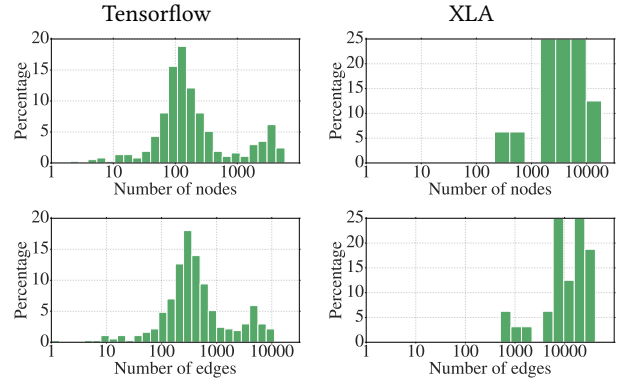


**Figure 3: Histograms of number of nodes and edges for the TensorFlow dataset (left) and XLA dataset (right).**

We augment the dataset by applying multiplicative noise to tensor sizes to create 100 variants per graph. Even though the variants from the same graph share the same topology, they represent 100 different peak memory minimization problem instances due to the different tensor sizes. The resulting dataset, denoted as the *TensorFlow dataset*, has 22400 training, 7400 validation, and 7400 test graphs. See details in section A.1.

As a more challenging test of the learned policy’s generalization, we evaluate policies trained using the TensorFlow dataset on 32 XLA graphs used by a production compiler team as a performance benchmark. This dataset presents two generalization challenges:

- XLA graphs use a different set of ops from TensorFlow and therefore the same model’s XLA and TensorFlow graphs can be significantly different. So we do not expect a priori that XLA graphs have the same distribution as TensorFlow graphs.
- Graphs in the benchmark have on average  $8.79\times$  more nodes and  $13.26\times$  more edges than those in the training set, and therefore the policy has to generalize to larger graph sizes.

We use the XLA graphs, denoted as the *XLA dataset*, as an additional test set. Figure 3 (right column) gives statistics for the number of nodes and edges.

### 4.2 Baselines

We use the following methods as baselines for comparison with REGAL.

*CP-SAT:* Constraint Programming (CP) is a widely used technique for scheduling problems (see, e.g., [19]). We use a SAT-based CP approach, implemented with Google OR-Tools [13]. The multi-device peak memory minimization problem is formulated for the CP solver using a model of the operation execution order, tensor lifetimes, and cumulative constraints to evaluate peak memory usage. The solver is guaranteed to find the globally optimal solution given sufficient time. We use a 12-hour time limit for the solve.

*Graph Partitioning + Depth First Search (GP+DFS):* This is a combination of the graph partitioning (GP) baseline for device placement in [22] and a Depth-First Search heuristic similar to the one

implemented in XLA to compute per-device schedules given placements. The graph partitioning objective is to minimize data transferred across devices. We use the modified implementation of the Kernighan-Lin [17] algorithm used by XLA for device placement in some settings. This implementation is generally slower than heuristics implemented in popular libraries like METIS [16] although it tends to find better quality solutions.

*Local Search:* Start with a random solution and greedily improve it by applying the best one-step look-ahead local move at each step. The initial schedule is a topological sort order of the ops, and the initial placement selects devices uniformly randomly. A local move either changes the device assignment of the op, or changes the op order in the current schedule. The hyperparameters (e.g., number of random restarts) are set to values that perform the best on a sample of 10,000 graphs in the training set as found by grid search.

*Graph-As-Sequence Model (GAS):* Like [21, 22], we convert the graph into a sequence using a topological sort and apply a recurrent neural network to predict node-level distributions to be used by BRKGA. This comparison measures the usefulness of graph structure for learning.

*BRKGA XK:* We run BRKGA for X thousand iterations with uniform sampling distributions using hyperparameters consistent with the recommendations in [12]:  $\pi = 100, \pi_e = 10, \pi_c = 80, \rho = 0.7$ . We diverge from [12] only by not scaling  $\pi$  with the chromosome size.

*Tuned BRKGA:* We tune the following hyperparameters of BRKGA using grid search: the elite bias parameter, the Beta distribution parameters (two scalars), and the number of chromosomes, elites, mutants, and populations. The grid search tries 648 hyperparameter settings and picks the best one as evaluated on 10,000 training set graphs.

For Local Search, GAS, Tuned BRKGA, and REGAL, we use the same limit on the number of objective evaluations allowed per graph to make the comparison fair. In our application setting, 5000 evaluations is possible within an acceptable running time, so we use that as the limit.

### 4.3 Comparison to baseline algorithms

We use two metrics to compare algorithms:

- *Average percent improvement over BRKGA 5K:* For a given graph, compute the percent improvement in peak memory achieved by an algorithm relative to running BRKGA with evaluation limit 5000.
- *Average percent gap from best known solution:* For a given graph, run CP SAT with a 24 hour time limit to compute the globally optimal peak memory. If CP SAT does not find the global optimum in the time limit, compute the best known peak memory value among all the algorithms. Compute the percent difference between an algorithm’s solution and the best known peak memory. On the TensorFlow test set, CP SAT solved 76.27% of the graphs optimally. On the XLA set, 6.25% were solved optimally.

Table 1 compares REGAL to other algorithms on the TensorFlow test set and the XLA dataset. On the TensorFlow test set, REGAL gives by far the biggest average improvement over BRKGA

**Table 1: Performance for all methods, averaged over the graphs in the test set of the TensorFlow and XLA datasets.**

Algorithm	TensorFlow dataset (test)		XLA dataset	
	% Improv. over	% Gap from	% Improv. over	% Gap from
	BRKGA5K	best	BRKGA5K	best
CP SAT	-1.77%	13.89%	-47.14%	71.35%
GP + DFS	-6.51%	16.63%	-21.43%	39.86%
Local Search	0.63%	8.65%	-6.69%	21.98%
BRKGA 5K	0%	9.65%	0%	14.04%
Tuned BRKGA	0.8%	8.54%	0.452%	13.52%
GAS	0.16%	9.33%	-1.1%	15.36%
<b>REGAL</b>	<b>3.56%</b>	<b>4.44%</b>	<b>3.74%</b>	<b>9.40%</b>

5K among all algorithms. The next best algorithm, Tuned BRKGA, achieves about 4.4× smaller improvement. REGAL has the lowest average percent gap from the best known solution. BRKGA 5K’s gap is 9.65%, while REGAL’s is 4.44%, so the addition of the learned policy captures approximately half of the headroom for improvement over BRKGA 5K.

On the XLA benchmark, REGAL is again the best with an even bigger average improvement over BRKGA 5K. This is a remarkable result considering the generalization challenges described in section 4.1. Other algorithms, in particular CP SAT, GP + DFS, and Local Search, become significantly worse, indicating that they are not able to handle the larger scale graphs. REGAL captures approximately one third of the headroom for improvement over BRKGA 5K, as the average percent gap from the best solution reduces from 14.04% for BRKGA 5K to 9.40% for REGAL.

REGAL’s strong results show that the learned policy a) successfully generalizes to previously unseen TensorFlow graphs and even XLA graphs, and b) substantially improves BRKGA’s search, to the extent that one-third to half of the estimated room for improvement over BRKGA 5K is captured using the *same* evaluation limit.

*4.3.1 Running time comparison:* Table 2 shows the average running times of the various algorithms on the TensorFlow test set and the XLA dataset, as measured on an Intel Xeon E5-1650 3.60GHz machine. The times are averaged over the unaugmented graphs in the test set. REGAL provides both fast running time as well as high solution quality. For a slightly higher running time than BRKGA 5K, REGAL improves the solution quality significantly. Almost all of the added running time is due to extra cost of sampling beta distributions by REGAL compared to uniform distributions by BRKGA. This can be seen from the nearly identical running times of REGAL and Tuned BRKGA, which also uses beta distributions, but without the neural network policy. The local search heuristic runs slowly because it was not implemented efficiently, e.g., with incremental evaluations of the objective; we show its timing results for completeness only.

### 4.4 Comparing REGAL vs. BRKGA

We compare REGAL more closely to BRKGA to understand how the learned policy helps. Figure 4 shows histograms of percent

[https://github.com/tensorflow/tensorflow/blob/4bfa2359152e9d106c2c20e9fff67643c8578e81/tensorflow/compiler/xla/service/hlo\\_memory\\_scheduler.h#L53](https://github.com/tensorflow/tensorflow/blob/4bfa2359152e9d106c2c20e9fff67643c8578e81/tensorflow/compiler/xla/service/hlo_memory_scheduler.h#L53)

**Table 2: Average running times for all methods.**

Algorithm	TensorFlow dataset (test)	XLA dataset
CP SAT	~2 hours	12+ hours
GP + DFS	144 sec	500 sec
Local Search	122 sec	1343 sec
BRKGA 5K	0.89 sec	8.82 sec
Tuned BRKGA	1.04 sec	10.0 sec
GAS	1.04 sec	10.1 sec
REGAL	1.04 sec	10.1 sec

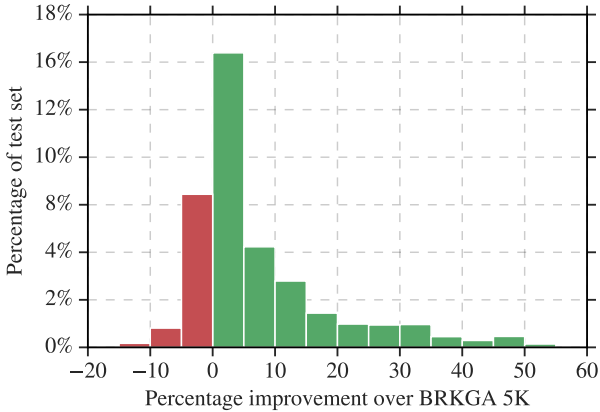


**Figure 4: Histogram of percent improvements in objective value for test graphs on which REGAL is better (green) and worse (red) than BRKGA**

improvements in peak memory achieved by REGAL on test dataset graphs. Green bars (on the right side of zero) correspond to graphs on which REGAL improved over BRKGA, while red bars (left of zero) correspond to graphs on which REGAL was worse. (Ties have been omitted for clarity.) REGAL matches or beats BRKGA on 88.92% of the TensorFlow test graphs. The highest improvement it achieves is 54.3%. On the 11.22% of test graphs where it performs worse than BRKGA, the worst regression is a peak memory increase of 17.9%. But most regressions are much smaller.

To assess whether the improvements provided by REGAL’s policy generalize to evaluation limits other than the one for which it was trained, we varied the evaluation limit used by both BRKGA and REGAL at test time. The results are shown in figure 5. REGAL’s performance improves with more evaluations, confirming that the policy generalizes to higher evaluation limits. In other words, there exist node-level choices for the distributions used in BRKGA that perform well regardless of the evaluation limit, and REGAL learns to predict those choices. This is particularly useful in cases where the actual evaluation limit to use will be known only at test time, so that the same policy can be applied without re-training. Interestingly, even with 50,000 evaluations, BRKGA is not able to match REGAL’s performance with just 5000 evaluations.

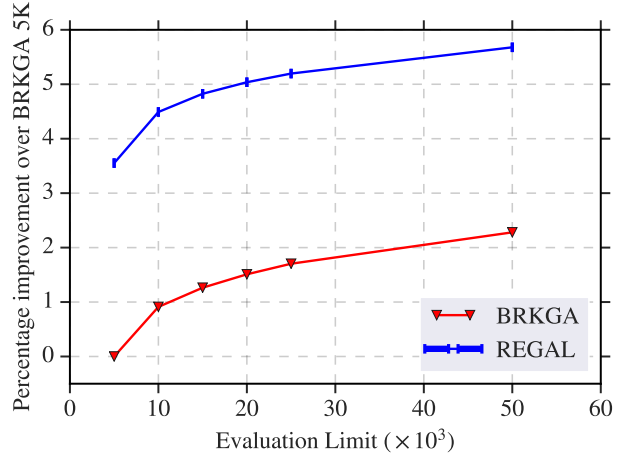


**Figure 5: Average percent improvement over BRKGA 5K given by REGAL and BRKGA on the TensorFlow test set as the evaluation limit is increased.**

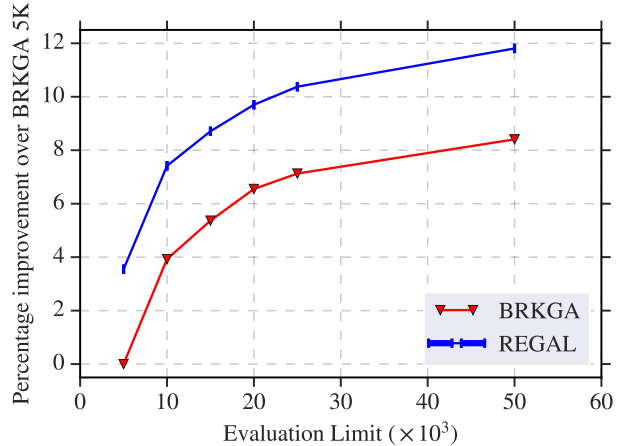


**Figure 6: Average percent improvement over BRKGA 5K given by REGAL and BRKGA on the XLA test set as the evaluation limit is increased.**

Figure 6 shows a similar result for the XLA dataset. Again, REGAL maintains its advantage over BRKGA at higher evaluation limits.

Another way to assess the policy’s effect on BRKGA is to evaluate the number of generations REGAL needs to match the objective value of BRKGA. For the 88.92% of test set graphs on which REGAL ties or improves BRKGA, it matches BRKGA on average in 47.8% fewer generations than BRKGA. This gives REGAL roughly half of the generations to spend on improving over BRKGA.

The performance of REGAL is stochastic both because the actions are stochastic and because BRKGA itself depends on random

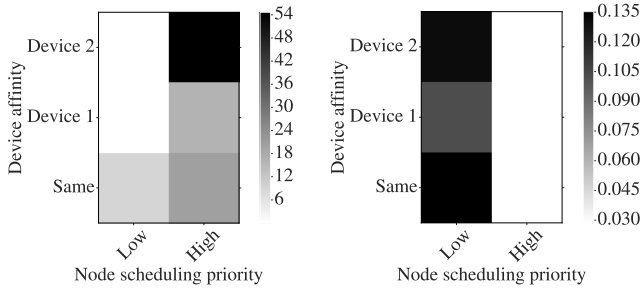


**Figure 7: The agent picks a diverse set of actions. These plots show the frequency of actions chosen (in percent, left) and the average relative weights of the nodes that the actions are applied to (right).**

samples for mutation and crossover. We estimated the standard deviation of the percent improvement statistics with respect to these sources of randomness as below 0.1%, which is small compared to the differences we observe. Hence we have omitted the error bars from figures 5 and 6.

## 5 ANALYSIS

In this section we analyze the behavior of the learned policy in more detail to gain insights into its performance.

### 5.1 Graph-dependent distribution choices

Our best model is capable of generating 16 different kinds of actions for node placement decisions and 4 different kind of actions for node scheduling decisions. Each of these actions determine the shape of the Beta distributions from which we sample the node-device affinities and the node scheduling priorities. Of the 16 placement actions, 6 actions give a node a higher probability to be placed on device 1, 6 actions give a node a higher probability to be placed on device 2, and the remaining 4 assign no preference to either of the devices. Among the 4 scheduling actions, 2 assign higher expected priority than the other 2. We aggregate these actions and present them in figure 7. Additionally, we aggregate the average relative memory consumption of all nodes that were assigned the same set of actions, where memory consumption of a node is defined as the sum of the memory uses of all its input and output tensors. The relative memory usage is the memory usage normalized by the largest memory usage of a node in the graph. We can observe that REGAL’s actions are non-trivially dependent on the input graph.

We observe that, on average, nodes with higher normalized memory consumption are assigned lower scheduling priorities. Moreover, most of the the nodes with the highest relative memory consumption have no affinity for either of the two devices. We also observe that among nodes with the lowest relative memory consumption, most of them have an affinity to be placed on device 2, while a smaller but still significant number of them prefer device 1. This implies that the node placement strategy is more complicated than a trivial "place lighter nodes on device 2" strategy.

Although there are very few actions that give heavy nodes a strong preference for placement on one device over the other, the

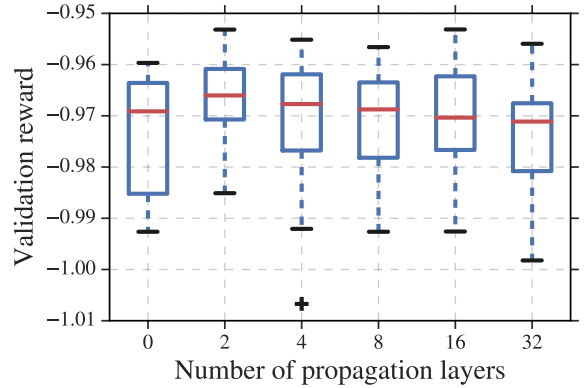


**Figure 8: Performance vs number of propagation layers in the GNN.**

ablation experiments in section 5.3 suggest that these placement actions are useful because they provide better generalization across the XLA dataset.

### 5.2 Use of graph structure

The policy makes non-trivial use of the graph structure in the input to achieve improved objective values.

We did a large sweep over 20 random seeds, baseline loss weights  $\lambda \in \{10^{-3}, 10^{-4}\}$ , and number of propagation layers in the graph neural network  $T \in \{0, 2, 4, 8, 16, 32\}$ . Figure 8 is a box plot showing how the policy’s performance on a fixed subset of 200 randomly selected computation graphs in the validation set (which we monitor during training) varies with respect to the number of propagation layers in the GNN. When the number of propagation layers is 0, the graph neural network ignores the graph structure in its inputs. As the number of propagation layers is increased, the network is able to use longer range graph information to make a prediction at each node.

We observe that there is a fair amount of variance in the results across random seeds and  $\lambda$  for each  $T$ . However, varying the number of propagation layers does affect the maximum achievable validation reward. In particular with no propagation layers, the policy does not reach a validation reward as high as possible for other  $T > 0$ . More over, when  $T = 0$  more runs end up with worse performance. On the other side, increasing  $T$  makes the model harder to train, see e.g. when  $T = 32$ , further increasing the variance in the results. Our best model was obtained with 16 propagation layers.

### 5.3 Ablation analysis of agent action types

REGAL can train a policy to generate any subset of the following actions for BRKGA:

- Actions for node placement priorities
- Actions for node scheduling priorities
- Actions for elite bias probabilities

We train REGAL with various subsets of these actions and compare their performance against each other in table 3. We observe that on the validation set, REGAL performs best when it has to learn

**Table 3: Performance of REGAL with various subsets of actions.**

Placement	Scheduling	Elite Bias	Valid	Test	XLA
Yes	No	No	-0.4%	-0.2%	-0.4%
No	Yes	No	4.4%	<b>3.65%</b>	1%
Yes	Yes	No	<b>4.67%</b>	3.56%	<b>3.74%</b>
Yes	No	Yes	-1.53%	-1.1%	-2.2%
No	Yes	Yes	2.47%	1.4%	-0.4%
Yes	Yes	Yes	2.58%	1.88%	-0.7%

actions for both placement and scheduling compared to just scheduling alone. Moreover, it performs even worse when it learns only node placement actions. Although the test set reward is higher for the agent that learns only scheduling actions, it performs worse on the XLA dataset compared to an agent that learns both placement and scheduling actions. This suggests that placement actions are much more important on the XLA dataset than on the test dataset.

We also observe that learning the elite bias probabilities gives worse performance compared to corresponding agents that don't learn elite bias actions.

## 6 CONCLUSIONS AND FUTURE WORK

By training a neural network policy to predict graph-conditional node distributions for BRKGA, REGAL successfully transfers to new graphs and significantly improves on BRKGA. Its added running time cost is marginal. REGAL's speed and generalization make it a strong choice for use in a production compiler that handles a diverse set of graphs and has a limited time budget.

We would like to explore the use of mixture modelling to further improve REGAL's performance. Given the diversity of graphs, a mixture model can train specialized sub-models on different types of graphs (e.g., convolutional networks, recurrent networks, etc.).

Finally, we can further extend REGAL in many directions:

- Optimize other execution costs, such as running time, and other types of decision variables, e.g., fusing ops in XLA graphs.
- Learn a sequential decision policy to be used within BRKGA's inner loop. By adapting its decisions as BRKGA is running on a graph, such a policy can potentially give even bigger gains.
- Extend beyond BRKGA and consider other optimizers, such as local search.

## ACKNOWLEDGMENTS

The authors would like to thank Ross Anderson, David Applegate, and Peter Hawkins for a significant amount of infrastructure on which this work builds, in particular the BRKGA and CP-SAT solutions to the multi-device peak memory minimization problem and the generation of the XLA dataset.

## REFERENCES

[1] Ravichandra Addanki, Shailesh Venkatakrishnan, Shreyan Gupta, Hongzi Mao, and Mohammad Alizadeh. 2018. Placeto: Efficient Progressive Device Placement Optimization. In *Workshop on ML for Systems at NeurIPS 2018*.

[2] The TensorFlow Authors. 2016. TensorFlow: Large-Scale Machine Learning on Heterogeneous Distributed Systems. *CoRR* abs/1603.04467 (2016). arXiv:1603.04467 <http://arxiv.org/abs/1603.04467>

[3] Yoshua Bengio, Andrea Lodi, and Antoine Prouvost. 2018. Machine Learning for Combinatorial Optimization: a Methodological Tour d'Horizon. *CoRR* abs/1811.06128 (2018). arXiv:1811.06128 <http://arxiv.org/abs/1811.06128>

[4] Matthias Boehm, Berthold Reinwald, Dylan Hutchison, Prithviraj Sen, Alexandre V. Evfimievski, and Niketan Parsare. 2018. On Optimizing Operator Fusion Plans for Large-scale Machine Learning in systemML. *Proc. VLDB Endow.* 11, 12 (Aug. 2018), 1755–1768. <https://doi.org/10.14778/3229863.3229865>

[5] Rudy Bunel, Alban Desmaison, M. Pawan Kumar, Philip H. S. Torr, and Pushmeet Kohli. 2017. Learning to superoptimize programs. In *International Conference on Learning Representations*.

[6] Tianqi Chen, Mu Li, Yutian Li, Min Lin, Naiyan Wang, Minjie Wang, Tianjun Xiao, Bing Xu, Chiyuan Zhang, and Zheng Zhang. 2015. Mxnet: A flexible and efficient machine learning library for heterogeneous distributed systems. *arXiv preprint arXiv:1512.01274* (2015).

[7] Tianqi Chen, Thierry Moreau, Ziheng Jiang, Lianmin Zheng, Eddie Yan, Meghan Cowan, Haichen Shen, Leyuan Wang, Yuwei Hu, Luis Ceze, Carlos Guestrin, and Arvind Krishnamurthy. 2018. TVM: An Automated End-to-End Optimizing Compiler for Deep Learning. In *OSDI 2018*.

[8] Tianqi Chen, Bing Xu, Chiyuan Zhang, and Carlos Guestrin. 2016. Training Deep Nets with Sublinear Memory Cost. *CoRR* (2016). <http://arxiv.org/abs/1604.06174>

[9] Tianqi Chen, Lianmin Zheng, Eddie Yan, Ziheng Jiang, Thierry Moreau, Luis Ceze, Carlos Guestrin, and Arvind Krishnamurthy. 2018. Learning to Optimize Tensor Programs. In *Neural Information Processing Systems 2018*.

[10] Peter W. Battaglia et al. 2018. Relational inductive biases, deep learning, and graph networks. *CoRR* (2018). arXiv:1806.01261 <http://arxiv.org/abs/1806.01261>

[11] Justin Gilmer, Samuel S Schoenholz, Patrick F Riley, Oriol Vinyals, and George E Dahl. 2017. Neural message passing for quantum chemistry. *arXiv preprint arXiv:1704.01212* (2017).

[12] José Fernando Gonçalves and Mauricio G. Resende. 2011. Biased Random-key Genetic Algorithms for Combinatorial Optimization. *Journal of Heuristics* 17, 5 (Oct. 2011), 487–525.

[13] Google. 2019. CP-SAT Solver. [https://developers.google.com/optimization/cp/cp\\_solver](https://developers.google.com/optimization/cp/cp_solver). [Online; accessed 21-January-2019].

[14] Sepp Hochreiter and Jürgen Schmidhuber. 1997. Long short-term memory. *Neural computation* 9, 8 (1997), 1735–1780.

[15] Zhihao Jia, Matei Zaharia, and Alex Aiken. 2018. Beyond Data and Model Parallelism for Deep Neural Networks. *CoRR* (2018). <http://arxiv.org/abs/1807.05358>

[16] G. Karypis and V. Kumar. 1998. A Fast and High Quality Multilevel Scheme for Partitioning Irregular Graphs. *SIAM Journal on Scientific Computing* 20, 1 (1998), 359–392.

[17] B. W. Kernighan and S. Lin. 1970. An efficient heuristic procedure for partitioning graphs. *The Bell System Technical Journal* 49, 2 (1970), 291–307.

[18] Yu-Kwong Kwok and Ishaq Ahmad. 1999. Static Scheduling Algorithms for Allocating Directed Task Graphs to Multiprocessors. *ACM Comput. Surv.* 31, 4 (Dec. 1999), 406–471.

[19] Philippe Laborie, Jérôme Rogerie, Paul Shaw, and Petr Vilim. 2018. IBM ILOG CP optimizer for scheduling. *Constraints* 23, 2 (01 Apr 2018), 210–250.

[20] Yujia Li, Daniel Tarlow, Marc Brockschmidt, and Richard Zemel. 2015. Gated graph sequence neural networks. *arXiv preprint arXiv:1511.05493* (2015).

[21] Azalia Mirhoseini, Anna Goldie, Hieu Pham, Benoit Steiner, Quoc V. Le, and Jeff Dean. 2018. A Hierarchical Model for Device Placement. In *International Conference on Learning Representations*. <https://openreview.net/forum?id=Hkc-TeZ0W>

[22] Azalia Mirhoseini, Hieu Pham, Quoc V. Le, Benoit Steiner, Rasmus Larsen, Yuefeng Zhou, Naveen Kumar, Mohammad Norouzi, Samy Bengio, and Jeff Dean. 2017. Device Placement Optimization with Reinforcement Learning. In *Proceedings of the 34th International Conference on Machine Learning, ICML 2017, Sydney, NSW, Australia, 6-11 August 2017*. 2430–2439.

[23] Brooks Paige and Frank Wood. 2016. Inference Networks for Sequential Monte Carlo in Graphical Models. In *Proceedings of the 33rd International Conference on International Conference on Machine Learning - Volume 48*.

[24] Razvan Pascanu, Tomas Mikolov, and Yoshua Bengio. 2013. On the difficulty of training recurrent neural networks. In *International Conference on Machine Learning*. 1310–1318.

[25] Adam Paszke, Sam Gross, Soumith Chintala, Gregory Chanan, Edward Yang, Zachary DeVito, Zeming Lin, Alban Desmaison, Luca Antiga, and Adam Lerer. 2017. Automatic differentiation in PyTorch. (2017).

[26] Nadav Rotem, Jordan Fix, Saleem Abdulrasool, Summer Deng, Roman Dzhabarov, James Hegeman, Roman Levenstein, Bert Maher, Nadathur Satish, Jakob Olesen, Jongsoo Park, Artem Rakhov, and Misha Smelyanskiy. 2018. Glow: Graph Lowering Compiler Techniques for Neural Networks. *CoRR* (2018). <http://arxiv.org/abs/1805.00907>

[27] Franco Scarselli, Marco Gori, Ah Chung Tsoi, Markus Hagenbuchner, and Gabriele Monfardini. 2009. The graph neural network model. *IEEE Transactions on Neural Networks* 20, 1 (2009), 61–80.

- [28] Eric Schkufza, Rahul Sharma, and Alex Aiken. 2013. Stochastic Superoptimization. (2013).
- [29] O. Sinnens. 2007. *Task Scheduling for Parallel Systems*. Wiley.
- [30] The XLA team. 2017. XLA - TensorFlow compiled. Post in the Google Developers Blog. <http://web.archive.org/web/20170308172654/https://developers.googleblog.com/2017/03/xla-tensorflow-compiled.html>.
- [31] Ronald J. Williams. 1992. Simple Statistical Gradient-Following Algorithms for Connectionist Reinforcement Learning. *Mach. Learn.* 8, 3-4 (1992), 229–256.
- [32] Yuan Yu, Martin Abadi, Paul Barham, Eugene Brevdo, Mike Burrows, Andy Davis, Jeff Dean, Sanjay Ghemawat, Tim Harley, Peter Hawkins, Michael Isard, Manjunath Kudlur, Rajat Monga, Derek Gordon Murray, and Xiaoqiang Zheng. 2018. Dynamic Control Flow in Large-Scale Machine Learning. *CoRR* (2018). <http://arxiv.org/abs/1805.01772>

## A APPENDIX

### A.1 Details of dataset creation

We collected a dataset by analyzing jobs running in a shared production cluster and extracting computation graphs in the MetaGraphDef format. As lots of computation graphs were repeated due to device or job replicas, we deduplicate the dataset by graph topology.

Computational costs for these computation graphs are simulated with an in-house simulator (based on Grappler) that outputs memory profiled information in the CostGraphDef format. The simulator TensorFlow Op coverage didn't include custom kernels or complicated control flow [32] like cycles (e.g. `tf.WhileLoop`).

The train-validation-test set split is made by selecting a set of 5 graphs from a list of graphs sorted by number of nodes, and splitting them as 3-1-1 across the three sets, respectively. This ensures that the distribution of the number of nodes is similar for the three sets.

For each graph in the train/validation/test sets, we make 99 copies of it and multiply each tensor size with a uniform sampled number in the interval (0.5, 1.5) (one sample per tensor size per copy). The modified copies are added back to the respective set so that the graph topologies in train/validation/test do not overlap.

We consider "control dependencies" as being tensors of size zero: Each triple (Op producer, tensor, Op consumer) in the CostGraphDef is encoded as a separate edge with the size of the tensor as a feature, meaning that the graph neural network input is a directed graph with parallel edges.

As node features we use the sum of input tensor sizes, the sum of output tensor sizes, the extra internal memory of the TensorFlow Op, and a node aggregation (the expectation of the placement per device and the schedule order for each node) of the chromosomes found by BRKGA running for 400 evaluations with uniform random distributions. To make comparisons fair, REGAL with  $K$  fitness evaluations means 400 evaluations to compute features, and  $K - 400$  fitness evaluations for BRKGA using the instance-specific distributions. For each graph, all node or edge features relating to memory size are normalized by the greatest memory size number in that graph.

To break symmetry we fix the placement of the node with highest memory to the first device and also add a node feature of 1 for that node and 0 otherwise.

### A.2 Action dequantization

To provide custom Beta distributions to BRKGA, the RL agent must generate two positive real numbers per distribution -  $\alpha$  and  $\beta$ . These two numbers parameterize a unique Beta distribution. To make the learning task easier, we quantize the output space of the RL agent's actions such that each action uniquely maps to a Beta distribution. This mapping is done as follows:

- For each Beta distribution, the agent must generate two integers  $m, v \in \{0, 1, \dots, k - 1\}$  where  $k$  is some fixed constant greater than 1.

- $m$  and  $v$  represent the quantized mean  $\mu$  and variance  $\sigma^2$  of some Beta distribution which are related to each other as follows:

$$\mu = \frac{m + 1}{k + 1}, \quad \sigma^2 = \mu \times (1 - \mu) \times \frac{v + 1}{k + 1}$$

- $\mu$  and  $\sigma^2$  can be mapped to  $\alpha$  and  $\beta$  as follows:

$$\beta = \mu \times \frac{(1 - \mu)^2}{\sigma^2} - 1 + \mu, \quad \alpha = \beta * \frac{\mu}{1 - \mu}$$

We use a similar quantization strategy for the crossover probabilities. For every crossover probability, we sample an integer  $c \in \{0, 1, \dots, k - 1\}$  from a Categorical distribution for some fixed integer constant  $k$ , and the crossover probability is dequantized by the formula `cross_over = 0.5 * (1 + c/k)`

### A.3 Extra model details

*MLPs.* Multi-layer perceptrons, or multi-layer fully connected neural networks are models that map input vectors to output vectors through layers of linear transformations and nonlinear activation functions, like the following:

$$\mathbf{h} = \text{MLP}(\mathbf{x}) = \mathbf{W}_l \sigma_{l-1} (\dots \sigma_2 (\mathbf{W}_2 \sigma_1 (\mathbf{W}_1 \mathbf{x} + \mathbf{b}_1) + \mathbf{b}_2)) \dots) + \mathbf{b}_l, \quad (10)$$

where  $\mathbf{x}$  is an input vector,  $(\mathbf{W}_i, \mathbf{b}_i)$  are the parameters for the  $i$ th layer, and  $\mathbf{h}$  is the output vector.  $\sigma$  is a nonlinear scalar function applied element-wise to the input vectors. Typical choices include the logistic sigmoid function  $\sigma(x) = \frac{1}{1+e^{-x}}$ , tanh function  $\sigma(x) = \frac{e^x + e^{-x}}{e^x - e^{-x}}$  and the ReLU function  $\sigma(x) = \max\{0, x\}$ .

*RNNs and LSTMs.* Recurrent neural networks (RNNs) are good sequence models. Typical RNNs contains a recurrent memory  $\mathbf{c}_t$  that is updated recursively by taking some input at each step  $t$  as the following:

$$\mathbf{c}_t = \text{RNNCell}(\mathbf{c}_{t-1}, \mathbf{x}_t), \quad (11)$$

where  $\mathbf{x}_t$  is the input at step  $t$ . The simplest RNN cell has the following form

$$\mathbf{c}_t = \sigma(\mathbf{W}[\mathbf{c}_{t-1}, \mathbf{x}_t] + \mathbf{b}), \quad (12)$$

where  $\mathbf{W}, \mathbf{b}$  are the parameters and  $\sigma$  is a nonlinearity.

Long-short term memory (LSTM) models are a type of RNNs that uses explicit gating to control the access to the memory. LSTMs distinguish the memory  $\mathbf{c}_t$  and the output of the LSTM  $\mathbf{h}_t$  as two sets of vectors, and compute the update at step  $t$  as

$$\mathbf{i} = \text{sigmoid}(\mathbf{W}_i[\mathbf{h}_{t-1}, \mathbf{x}_t] + \mathbf{b}_i) \quad (13)$$

$$\mathbf{f} = \text{sigmoid}(\mathbf{W}_f[\mathbf{h}_{t-1}, \mathbf{x}_t] + \mathbf{b}_f) \quad (14)$$

$$\mathbf{o} = \text{sigmoid}(\mathbf{W}_o[\mathbf{h}_{t-1}, \mathbf{x}_t] + \mathbf{b}_o) \quad (15)$$

$$\mathbf{g} = \tanh(\mathbf{W}_g[\mathbf{h}_{t-1}, \mathbf{x}_t] + \mathbf{b}_g) \quad (16)$$

$$\mathbf{c}_t = \mathbf{f} \odot \mathbf{c}_{t-1} + \mathbf{i} \odot \mathbf{g} \quad (17)$$

$$\mathbf{h}_t = \mathbf{o} \odot \tanh(\mathbf{c}_t). \quad (18)$$

Here  $\mathbf{i}, \mathbf{f}, \mathbf{o}$  are the input, forget and output gates and  $\odot$  is element-wise multiplication. The carefully designed memory access control through gating makes LSTMs better at modeling long-term dependencies.

[https://github.com/tensorflow/tensorflow/blob/68052b3303153c4e2ada0865e93bb3f9e729ba13/tensorflow/core/protobuf/meta\\_graph.proto](https://github.com/tensorflow/tensorflow/blob/68052b3303153c4e2ada0865e93bb3f9e729ba13/tensorflow/core/protobuf/meta_graph.proto)  
<https://github.com/tensorflow/tensorflow/blob/68052b3303153c4e2ada0865e93bb3f9e729ba13/tensorflow/core/grappler>  
[https://github.com/tensorflow/tensorflow/blob/68052b3303153c4e2ada0865e93bb3f9e729ba13/tensorflow/core/framework/cost\\_graph.proto](https://github.com/tensorflow/tensorflow/blob/68052b3303153c4e2ada0865e93bb3f9e729ba13/tensorflow/core/framework/cost_graph.proto)

### A.4 Placement and scheduling example

Figure 9 illustrates a computation graph, a valid schedule, and how we account for which tensors are in memory at a given time under the model presented in sec. 3.1.

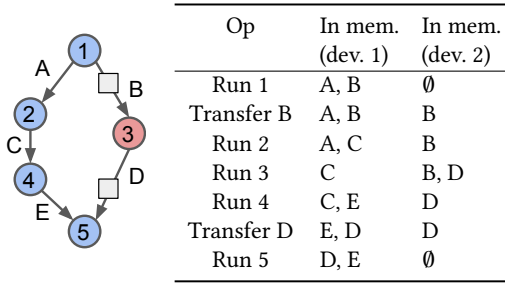


Figure 9: An example computation graph and execution schedule across two devices. Op 3 is assigned to device 2 while all others are assigned to device 1.

### A.5 Hyperparameters of the best model

The graph neural network had a state size of 32 for each node and edge, 16 propagations, all networks  $MLP_n$   $MLP_e$   $MLP_{node}$   $MLP_{msg}$   $MLP'_{msg}$  being two layers of size 32, the aggregation used was mean pooling. For faster training, the reward of the training set was made with 1000 fitness evaluations for REGAL and BRKGA (4600 for REGAL and 5000 for BRKGA for the validation and test sets). Training lasted 100000 gradient steps with each step having a mini-batch of size 4 and with gradient clipping by  $L_2$  norm with value 10. The baseline mean squared error term's contribution to the overall loss was weighted by 0.0001. The optimizer was Adam with beta1 0.9 beta2 0.999 epsilon  $1e-8$  and learning rate 0.0001. The number of devices (for the memory model) was 2.